LAWRENCE
LIVERMORE
NATIONAL
LABORATORY

UCRL-CONF-227192

# Rayleigh-Taylor instability-induced mixing: initial conditions modeling, three-dimensional simulations and comparisons with experiment

N. Mueschke, O. Schilling, M. Andrews

January 11, 2007

International Workshop on the Physics of Compressible Turbulent Mixing
Paris, France
July 17, 2006 through July 21, 2006

e-mail: schilling1@llnl.gov

# Rayleigh–Taylor instability-induced mixing: initial conditions modeling, three-dimensional simulations and comparisons with experiment

Nicholas MUESCHKE[1], Oleg SCHILLING[2] and Malcolm ANDREWS[3]

[1] *Texas A&M University, College Station, Texas 77843, USA*
[2] *University of California, Lawrence Livermore National Laboratory, Livermore, California 94551, USA*
[3] *Los Alamos National Laboratory, Los Alamos, New Mexico 87545, USA*

**Abstract:** A spectral/compact finite-difference method with a third-order Adams–Bashforth–Moulton time-evolution scheme is used to perform a direct numerical simulation (DNS) of Rayleigh–Taylor flow. The initial conditions are modeled by parameterizing the multi-mode velocity and density perturbations measured just off of the splitter plate in water channel experiments. Parameters in the DNS are chosen to match the experiment as closely as possible. The early-time transition from a weakly-nonlinear to a strongly-nonlinear state, as well as the onset of turbulence, is examined by comparing the DNS and experimental results. The mixing layer width, molecular mixing parameter, vertical velocity variance, and density variance spectrum obtained from the DNS are shown to be in good agreement with the corresponding experimental values.

## 1 INTRODUCTION

The purpose of this research is to elucidate the physics of turbulent transport, and transitional dynamics in Rayleigh–Taylor instability-driven mixing layers using coupled experiments and high-resolution three-dimensional direct numerical simulations (DNS). To accomplish this, experimental measurements characterizing the initial conditions and the evolution of various large-scale and turbulence statistics were performed within a small Atwood number, incompressible, miscible Rayleigh–Taylor mixing layer [1,2]. A DNS model of the experiment was formulated using parameters that closely correspond to the experiment and experimentally-measured initial density and velocity perturbations. Data from this DNS was also used to investigate the relative importance of terms in the turbulent kinetic energy transport equation and the validity of the gradient-diffusion approximation in modeling these terms [3].

## 2 EXPERIMENTAL FOUNDATION

Measurements were taken is an open-loop water channel facility at Texas A&M University. A schematic of the water channel and the associated diagnostics can be found elsewhere [1,2]. An adverse density stratification was created by heating the bottom water stream. The temperature difference ($\Delta T \approx 5^{\circ}$C) created a density difference through thermal expansion of the bottom stream, resulting in an Atwood number $A = (\rho_1 - \rho_2)/(\rho_1 + \rho_2) \approx 7.5 \times 10^{-4}$. Downstream distance, $x$, is converted to time using Taylor's hypothesis and normalized such that $\tau = x/\left(U_m\sqrt{gA/H}\right)$, where $U_m = 4.5$ cm/s is the mean velocity of the water streams, $g = 981$ cm/s$^2$, and $H = 32$ cm is the height of the channel.

## 3 EQUATIONS SOLVED AND THE NUMERICAL METHOD

The DNS uses a hybrid spectral and tenth-order compact differencing spatial discretization scheme to solve the conservation of mass, momentum, and mass fraction evolution equations [4]:

$$\frac{\partial \rho}{\partial t} + \frac{\partial}{\partial x_j}(\rho\, u_j) = 0\,, \tag{3.1}$$

$$\frac{\partial}{\partial t}(\rho\, u_i) + \frac{\partial}{\partial x_j}(\rho\, u_i\, u_j) = \rho\, g_i - \frac{\partial p}{\partial x_i} + \frac{\partial \sigma_{ij}}{\partial x_j}\,, \tag{3.2}$$

$$\frac{\partial}{\partial t}(\rho\, m_r) + \frac{\partial}{\partial x_j}(\rho\, m_r\, u_j) = \frac{\partial}{\partial x_j}\left(\rho\, D\, \frac{\partial m_r}{\partial x_j}\right), \tag{3.3}$$

where $\rho$ is the density, $u_i$ is the velocity, $g_i$ is gravity, $p$ is the pressure, $\sigma_{ij} = \mu\,(\partial u_i/\partial x_j + \partial u_j/\partial x_i) - (2/3)\mu\delta_{ij}\partial u_k/\partial x_k$ is the viscous stress tensor [with $\mu = \rho\nu$ the dynamic viscosity and $\nu = (\mu_1 + \mu_2)/(\rho_1 + \rho_2)$ the constant kinematic viscosity], $m_r$ is the mass fraction of fluid $r = 1, 2$, and $D$ is the constant mass diffusivity. Time integration is performed using a third-order Adams–Bashforth–Moulton predictor-corrector scheme. The physical and numerical parameters are given in Table 3.1.

| Parameter | Value |
|---|---|
| $\rho_1$ | 0.9986 g/cm$^3$ |
| $\rho_2$ | 0.9970 g/cm$^3$ |
| $A$ | $7.5 \times 10^{-4}$ |
| $g_z$ | $-981$ cm/s$^2$ |
| $\mu_1$ | 0.009 g/(cm s) |
| $\mu_2$ | 0.011 g/(cm s) |
| $Pr$ ($\nu/D$ in DNS) | 7 |
| $L_x \times L_y \times L_z$ | 16 cm $\times$10 cm $\times$16 cm |
| $N_x \times N_y \times N_z$ | $384 \times 240 \times 512$ |

**Table 3.1.** Parameters used in the DNS of the water channel experiment.

## 4 THE MODEL OF THE INITIAL CONDITIONS

The initial interface between the two fluids in the DNS was parameterized by orthogonal perturbations in the $x$- and $y$-directions:

$$\zeta(x, y) = \sum_{k_x} \hat{\zeta}_x(k_x)\, \mathrm{e}^{ik_x x} + \sum_{k_y} \hat{\zeta}_y(k_y)\, \mathrm{e}^{ik_y y}, \tag{4.1}$$

where $k_x$ and $k_y$ are the perturbation wavenumbers. The initial velocity was constructed from a potential formulation, where the potential field is perturbed to give the measured initial vertical velocity fluctuations,

$$\phi_r(x, z) = \sum_{k_x} \frac{\hat{w}(k_x)}{k_x} \sin\left[k_x\, x + \varphi(k_x)\right] \mathrm{e}^{-k_x|z|}, \tag{4.2}$$

where $\varphi(k_x)$ are the phases. The initial velocity field is the gradient of the potential field. In Eqs. (4.1) and (4.2), the perturbation amplitudes $\hat{\zeta}_x(k_x)$, $\hat{\zeta}_y(k_y)$, and $\hat{w}(k_x)$ are taken directly from the corresponding experimentally-measured one-dimensional spectra [2]. The measured initial interfacial and velocity spectra from the water channel [1,2] are shown in Fig. 4.1 to illustrate the high degree of anisotropy at the onset of the instability.

## 5 COMPARISONS OF DNS RESULTS WITH EXPERIMENTAL DATA

### 5.1 Mixing Layer Growth

The evolution of the $f_1 = 0.5$ volume fraction isosurface is shown in Fig. 5.2. Qualitatively, the mixing layer growth is dominated by the initial velocity perturbations in the $x$-direction. The early ($\tau < 0.5$) structure of the mixing layer is predominantly two-dimensional, as observed in the experiments. For $\tau > 0.5$, perturbations to the initial density interface become important as the mixing layer dynamics become highly-nonlinear and more three-dimensional structure develops.

The mixing layer width is measured by the 5–95% thresholds of the volume fraction profiles. The evolution of the bubble and spike front penetrations is shown in Fig. 5.3. The DNS agrees fairly well with the mixing layer growth measurements of Snider [5] and Wilson [6]; however, the DNS grows slightly faster than the experiment, which may be due to the lack of statistical convergence in longer wavelengths. As the mixing layer develops, the dominant structures determining its growth become larger, and thus fewer exist within the finite computational domain.

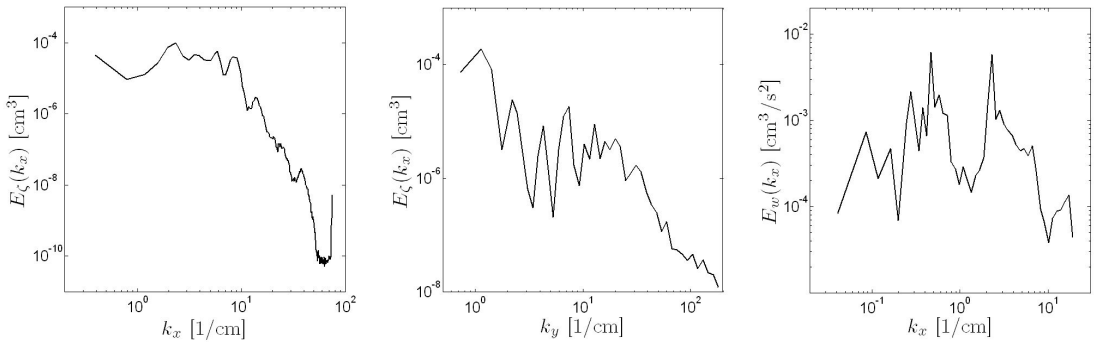


**Fig. 4.1.** The initial one-dimensional spectra for the DNS. Left: interfacial perturbations in the $x$-direction. Middle: interfacial perturbations in the $y$-direction. Right: vertical velocity fluctuations at the centerplane of mixing layer in the $x$-direction.

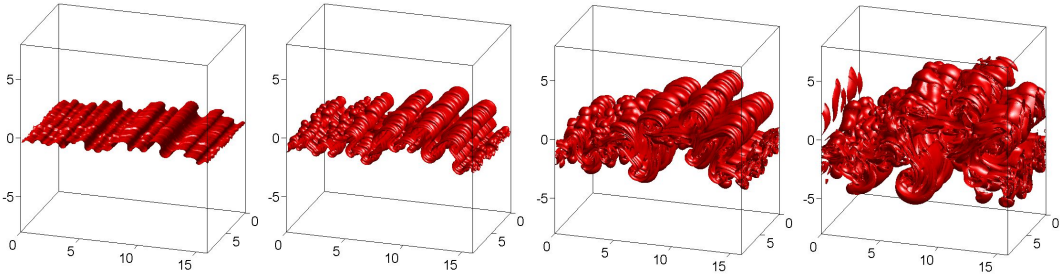

**Fig. 5.2.** The volume fraction $f_1 = 0.5$ isosurface at $\tau = 0.25, 0.50, 0.75, 1.00$.

Figure 5.3 also shows the evolution of the integral-scale Reynolds number of the DNS, where $Re = UL/\nu$ and $U$ and $L$ are characteristic velocity and lengthscales, respectively. The mixing layer width $h(t) = h_b(t) + h_s(t)$ is chosen as the lengthscale for all of the Reynolds numbers shown in Fig. 5.3. Various velocity scales have been used, including the total penetration rate of the mixing layer $\mathrm{d}h/\mathrm{d}t$, the terminal velocity of the dominant bubble diameter $v_\infty$, and the rms centerplane vertical velocity fluctuations $\overline{w'^2}$. Depending upon the velocity scale used, the final Reynolds number achieved in the DNS ranges from 1200–2000.

## 5.2 Turbulence and Mixing Statistics

In addition to comparisons of integral-scale quantities, turbulence and mixing statistics are also compared between the DNS and experiment. First, the degree of molecular mixing between the two fluids at the centerplane of the mixing layer, $\theta = 1 - \overline{f_1'^2}/(\overline{f_1}\,\overline{f_2})$, is compared, where $f_r$ is the volume fraction of fluid $r$ (all averages are taken at the centerplane). A value $\theta = 1$ indicates that the fluids are completely mixed, and $\theta = 0$

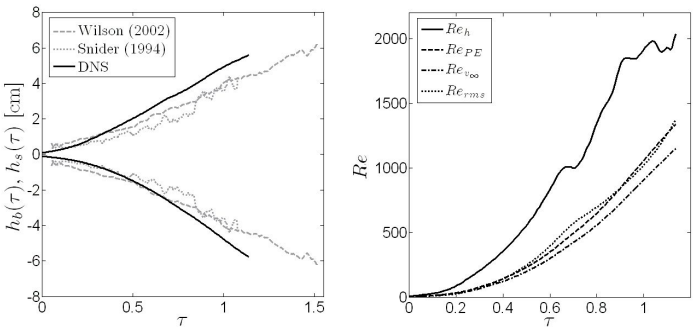


**Fig. 5.3.** The evolution of the bubble and spike fronts, $h_b$ and $h_s$, and integral-scale Reynolds number, $Re$.

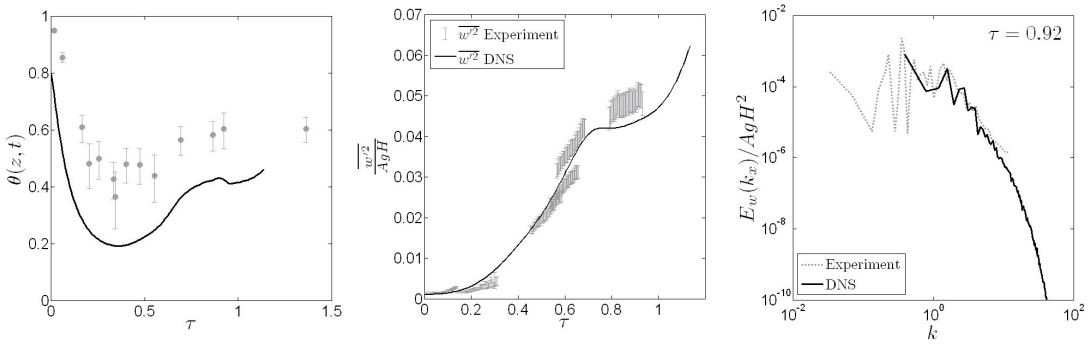


**Fig. 5.4.** Comparison of DNS results with the experimental measurements of $\theta$, the normalized vertical velocity variance, and the normalized density variance spectrum. Error bars are shown on the measurements of $\theta$ and the normalized vertical velocity variance.

indicates complete segregation. Values from the DNS and experiment are shown in Fig. 5.4. The DNS follows the experimentally measured trends closely, but underpredicts the total amount of mixed fluid. This may be associated with the method of implementing the initial velocity conditions and how energy from the initial spectrum is distributed among the discrete modes that can be supported on the computational grid.

The vertical velocity fluctuations at the centerplane of the mixing layer $\overline{w'^2}/(AgH)$ and the one-dimensional energy spectrum of the centerplane vertical velocity fluctuations $E_w(k_x)/\left(AgH^2\right)$ is shown at $\tau = 0.92$ from the DNS and experiment in Fig. 5.4. Both quantities compare very well. In particular, the DNS and experimental spectra agree quite well over the entire range of scales that overlap.

## 6 CONCLUSIONS

A DNS of a small Atwood number, multi-mode Rayleigh–Taylor mixing layer was initialized using interfacial and velocity perturbations parameterized from experimental measurements. Results from the DNS and experiment showed favorable agreement. Differences are attributed to details in the method of parameterizing the initial conditions, and the lack of statistical convergence at late time due to a limited computational domain size. Both of these are strongly related to the inclusion of longer wavelengths, which affect the integral-scale and turbulence statistics compared. A transition to highly-nonlinear dynamics was observed at $\tau \approx 0.4$, which was seen in the rapid increase of vertical velocity fluctuations and the increase in the degree of molecular mixing. This transition point and the magnitudes of $\overline{w'^2}$ and $\theta$ at this point were observed to be a function of the exact implementation of the initial conditions. Accordingly, higher resolution DNS investigating the effects of longer wavelengths on the quantities considered here are in progress.

This research was supported by the National Nuclear Security Administration under the Stewardship Science Academic Alliances program through DOE Research Grant #DE-FG03-02NA00060. This work was also performed under the auspices of the U.S. Department of Energy by the University of California Lawrence Livermore National Laboratory under contract No. W-7405-Eng-48.

## REFERENCES

[1] Mueschke, N. J., 2004. An Investigation of the Influence of Initial Conditions on Rayleigh–Taylor Mixing. M.S. thesis, Texas A&M University.

[2] Mueschke, N. J., Andrews, M. J. and Schilling O., 2006. Experimental characterization of initial conditions and spatio-temporal evolution of a small Atwood Rayleigh–Taylor mixing layer. *J. Fluid Mech.* **567**, pp. 27–63.

[3] Schilling, O., Mueschke, N. J. and Latini, M., 2007. Assessment of gradient-diffusion closures for modeling Rayleigh–Taylor and Richtmyer–Meshkov instability-induced mixing, in *Proceedings of the Tenth International Workshop on the Physics of Compressible Turbulent Mixing*, 17–21 July 2006, Paris, France, edited by M. Legrand and M. Vandenboomgaerde.

[4] Cook, A. W. and Dimotakis, P. E., 2001. Transition stages of Rayleigh–Taylor instability between miscible fluids. *J. Fluid Mech.* **443**, pp. 69–99. Corrigendum. *J. Fluid Mech.* **457**, pp. 410–411 (2002).

[5] Snider, D. M. and Andrews, M. J., 1994. Rayleigh–Taylor and shear driven mixing with an unstable thermal stratification. *Phys. Fluids A* **6**, pp. 3324–3334.

[6] Wilson, P. N., 2002. An Investigation into the Spectral Evolution of Turbulent Mixing by Rayleigh–Taylor Instability. Ph.D thesis, Texas A&M University.